Classifying Surfactants with Respect to Their Effect on Lipid Membrane Order

Mozhgan Nazari, Mustafa Kurdi, and Heiko Heerklotz*
Leslie Dan Faculty of Pharmacy, University of Toronto, Toronto, Ontario, Canada

ABSTRACT We propose classifying surfactants with respect to their effect on membrane order, which is derived from the time-resolved fluorescence anisotropy of DPH. This may help in understanding why certain surfactants, including biosurfactants such as antimicrobial lipopeptides and saponins, often show a superior performance to permeabilize and lyse membranes and/or a better suitability for membrane protein solubilization. Micelle-forming surfactants induce curvature stress in membranes that causes disordering and, finally, lysis. Typical detergents such as $C_{12}EO_8$, octyl glucoside, SDS, and lauryl maltoside initiate membrane lysis after reaching a substantial, apparently critical extent of disordering. In contrast, the fungicidal lipopeptides surfactin, fengycin, and iturin from *Bacillus subtilis* QST713 as well as digitonin, CHAPS, and lysophosphatidylcholine solubilize membranes without substantial, overall disordering. We hypothesize they disrupt the membrane locally due to a spontaneous segregation from the lipid and/or packing defects and refer to them as heterogeneously perturbing. This may account for enhanced activity, selectivity, and mutual synergism of antimicrobial biosurfactants and reduced destabilization of membrane proteins by CHAPS or digitonin. Triton shows the pattern of a segregating surfactant in the presence of cholesterol.

INTRODUCTION

Membrane lysis and solubilization by detergents and surfactantlike biomolecules is a key phenomenon in many biological functions and technical applications. The most prominent examples are the leakage and lysis of cell membranes by antibiotic (lipo)peptides (1) or antiseptic or spermicidal agents (2) and the isolation and study of membrane proteins (3).

The key property of a micelle-forming amphiphile inserting into a lipid bilayer is its preference for a locally curved interface (its spontaneous curvature) that is in conflict with the, on average, planar topology of a bilayer. This misfit causes a curvature stress, that is, a penalty to membrane excess enthalpy (4,5) and free energy (5,6) and a strain disordering and thinning the hydrophobic core of the membrane (7). Depending on the size and shape of their polar and apolar parts, detergents can be weak or strong in terms of inducing curvature stress (8) but nevertheless share the same principal mode of membrane solubilization. Similar excess enthalpies (5) and deuterium order parameters (9) at the onset of solubilization have led to the hypothesis of a critical curvature strain in the membrane that needs little (typically, some 20–40 mol %) of a strong or much (e.g., 60 mol %) of a weak detergent to be reached.

However, the fact that a variety of structural and kinetic pathways has been described for different lipid-detergent systems indicates that the state of such a system is not sufficiently determined by its average spontaneous curvature alone. Structural intermediates have been identified as wormlike micelles, perforated vesicles, or bilayer sheets and disks (10,11). Kragh-Hansen et al. (12) described two kinetic pathways—a transbilayer mechanism proceeding via membrane destruction by inserted detergents, and a micellar mechanism based on the appearance or persistence of micelles in solution that extract lipid from the membrane upon collisions. The usually slow, micellar mechanism may in particular apply to surfactants that cannot translocate quickly to the inner membrane leaflet; they give rise to a bilayer asymmetry stress that opposes further uptake and favors the release of molecules from the overpopulated outer leaflet (12,13).

Unspecific, detergentlike (14–16), or carpetlike (17) action has also been discussed to account for the membrane-permeabilizing activity of certain antimicrobial peptides. These molecules differ usually from the head-and-tail structure of detergents but they share with detergents their amphiphilic nature and the induction of curvature strain in membranes. This is revealed, for example, by their ability to inhibit the transition to inverse hexagonal (18,19) or induce a micellar cubic (Pm3n (20)) phase of a lipid. However, whereas such peptides form membrane defects and toroidal pores that are similar to those induced by detergents (21,22), they do so at much lower concentration and with superior selectivity.

This raises the question whether there is a principal difference between the effects of surfactants on membranes that is independent of spontaneous curvature and membrane permeability. We have addressed this question by testing the correlation between the lytic activity of surfactants with their impact on overall membrane order, which is directly related to curvature stress (see also Lafleur et al. (7)). After obtaining first hints from deuterium NMR (9), we have employed time-resolved fluorescence anisotropy measurements of DPH and two of its derivatives here. Briefly, the limiting anisotropy, r_∞, and rotational correlation time, θ, of the probes represent the order (constraints

Submitted July 19, 2011, and accepted for publication December 9, 2011.

*Correspondence: heiko.heerklotz@utoronto.ca

Editor: Klaus Gawrisch.

0006-3495/12/02/0498/9 $2.00

doi: 10.1016/j.bpj.2011.12.029

to molecular orientation) and dynamics (speed of rotational motion) in the membrane. In some interesting studies, particularly r_∞ was shown to quantify the disordering effect of detergents (2,23). Sýkora et al. (24) showed that digitonin retained a higher order as well as a better activity of a G-protein than synthetic detergents.

We should mention that the detailed interpretation of DPH fluorescence and anisotropy decays remains partially unclear or controversial in spite of extensive, sophisticated studies. For example, DPH was modeled to show a characteristic tilt with respect to the membrane normal (the classical wobble-in-cone model) or to tumble around the normal direction (Brownian rotational diffusion model) (25,26). DPH was argued to partition between two typical localizations in the membrane: 1), essentially parallel to the chains within a given leaflet, and 2), perpendicular to the chains between the two lipid leaflets (27). TMA-DPH, an analog with a cationic group at one end, cannot localize in the center of the membrane but might distribute between an inserted and interfacial orientation of the fluorophore (28). The fluorescence lifetime(s) of DPH are affected by the exposure to water and DPH self-quenching (29,30), but it is not straightforward to assign the two lifetimes to two specific localizations because the decay is biexponential even in an isotropic solvent (29). In membranes with fluid and gel-state domains, DPH partitions essentially equally between the phases but TMA-DPH and DPH-PC show a preference for the fluid phase (31).

In our case, the coexistence of (potentially heterogeneous) membranes and different types of micelles renders the physics of the fluorophore even more complex and a detailed fit is not warranted. However, it turns out that the comparison of the average (monoexponential) decay behavior of DPH, TMA-DPH, and DPH-labeled phospholipid (DPH-PC) in different systems and under different conditions provides much insight even on a partially empirical level. Fig. 1 shows the molecular dimensions of some of the molecules used in our study.

MATERIALS AND METHODS

Materials

Synthetic detergents $C_{12}EO_8$ (octaethylene glycol mono-dodecyl ether), OG (*n*-octyl β-D-glucopyranoside), TX (triton X-100), LM (lauryl maltoside, *n*-dodecyl-α-D-maltopyranoside), SDS (sodium dodecyl sulfate), CHAPS (3-[(3-cholamidopropyl)-dimethylammonio]-1-propane sulfonate), and lysoPC (1-lauroyl-2-hydroxy-3-phosphatidylcholine) were obtained from Anatrace (Maumee, OH) in Anagrade purity (99% high-performance liquid chromatography). Surfactins (SF), fengycins (FE), and iturins (IT) are classes of closely related lipopeptides (see Ongena and Jacques (1) for an overview) produced by *Bacillus subtilis* QST713 and were kindly provided by AgraQuest (Davis, CA). Digitonin was purchased from Wako Chemicals (Richmond, VA).

The lipid POPC (1-palmitoyl-2-oleoyl-*sn*-glycero-3-phosphocholine) was purchased from Avanti Polar Lipids (Alabaster, AL). The probes, DPH (1,6-diphenylhexatriene), TMA-DPH (1-(4-trimethylammonium-phenyl)-6-phenyl-1,3,5-hexatriene *p*-toluenesulfonate), and DPH-PC (2-(3-(diphenylhexatrienyl)propanoyl)-1-hexadecanoyl-*sn*-glycero-3-phosphocholine) were from Molecular Probes Invitrogen (Eugene, OR). NaCl (sodium chloride), Tris (tris(hydroxymethylo)-aminomethane), and EDTA (ethylenediaminetetraacetic acid) were from Sigma-Aldrich (St. Louis, MO) at the highest available purity. All samples were prepared in buffer containing 100 mM NaCl, 10 mM Tris, and 0.5 mM EDTA in Millipore water (Millipore, Billerica, MA), adjusted to pH 8.5.

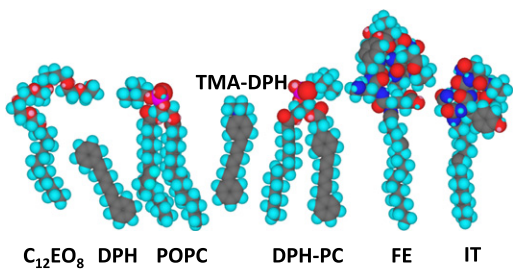

FIGURE 1 Illustration of the molecular dimensions of some molecules involved in the study.

Samples

Lipid vesicles were prepared as described elsewhere (32). For anisotropy experiments, the probe (DPH, TMA-DPH, or DPH-PC) was added to a solution of the lipid (POPC) in chloroform to establish a lipid/probe mole ratio of 1:600. The solution was dried by a gentle stream of nitrogen, followed by exposure to vacuum overnight. Then, the lipid was quantified gravimetrically assuming an effective molar weight including one bound water molecule per lipid (778 g/mol for POPC) as validated earlier by phosphorus assays. Multilamellar suspensions of lipid were prepared by adding buffer to each sample, vortexing, and six freeze-thaw cycles. Then, large unilamellar vesicles were prepared by extrusion through Nucleopore filters of ~100-nm pore size in a Lipex extruder (Northern Lipids, Burnaby, British Columbia, Canada). The large unilamellar vesicles had a size of ~100 nm as confirmed by dynamic light scattering. For isothermal titration calorimetry (ITC) experiments, the same protocol was followed without adding probe.

Fluorescence experiments

Typically, experimental series were carried out as titrations. Small amounts of a stock solution of detergent micelles were added (keeping lipid dilution small) sequentially to a starting sample of 2 mL, 2 mM lipid. For detergents known to undergo a fast flip-flop between the leaflets of the bilayer ($C_{12}EO_8$, TX, OG), the sample was stirred for 15 min after each injection for equilibration. In series studying the other surfactants, the equilibration was realized for at least 15 min at 65°C followed by readjustment of the experimental temperature, 20°C. This procedure was based on the finding that this temperature renders POPC membranes permeable even for charged surfactants such as SDS ((33), unpublished data for alkyl maltosides). Series with individual samples and 1 h heat treatments as well as spot checks with lipid and surfactant premixed in chloroform before extrusion yielded no significant deviations.

Time-resolved anisotropy decays were recorded at 20.0°C on a FL3 system (Horiba Scientific, Edison, NJ) utilizing time-correlated single photon counting. Source of excitation was 340 nm LED pulsed at 1 MHz, and emission was detected at 425 nm (slit 5 nm, double-grated monochromator) by a TBX detector (Horiba Scientific). Fluorescence decays were recorded with horizontal and perpendicular orientations of polarizers in the excitation and emission path, with automatic cycling between the emission polarizer orientations every 60 s. The instrument response function was recorded with a dilute Ludox scattering dispersion.

The data evaluation utilized in DAS 6 software (Horiba Scientific) follows a similar strategy to the one explained by Lakowicz (34). Briefly, the fluorescence decays were analyzed by deconvoluting the sum of curves obtained with the vertical and horizontal polarizer, I_{VV} and I_{VH}, with the instrument response function using a biexponential decay model, considering the G-factor. Typical values of χ^2 were 1.5. Then, the difference signal was deconvoluted with the exponential decay function obtained for the sum signal to obtain the parameters of a monoexponential anisotropy decay function,

$$r(t) = [r_0 - r_\infty]\cdot\exp\left\{-\frac{t}{\theta}\right\} + r_\infty, \qquad (1)$$

where the rotational correlation time, θ, reflects the dynamics of the reorientation of the probe. The limiting anisotropy, r_∞, reflects constraints to the motion of the probe and is related to membrane order. As discussed above, the monoexponential model was chosen for the sake of stability, even if nonrandom residuals were observed. The time window of the fit was ≈2400 channels (67 ns).

Other techniques

Isothermal titration calorimetry (ITC) was performed as described elsewhere (32) using a VP ITC (MicroCal, Northampton MA). For the solubilization experiment, the syringe is loaded with a relatively highly concentrated, micellar solution of the surfactant (150 mM of OG in the example shown) and a series of injections is carried out into the calorimeter cell (≈1.5 mL) originally filled with a 2 mM dispersion of POPC vesicles. The onset and completion of solubilization become visible as break points of the normalized heat of titration. Injection volumes were varied between 2 and 15 μL and waiting times after each injection were set to 40 min to ensure complete equilibration.

Dynamic light scattering as shown for SF-POPC mixtures was done in a Nano ZS system (Malvern Instruments, Malvern, UK), utilizing noninvasive backscattering at 173° at a wavelength of 633 nm. The measurements were done with the samples used for the DPH experiments before.

RESULTS

Fig. 2 illustrates the effects of the detergent $C_{12}EO_8$ on the order and dynamics of POPC membranes in terms of the decay parameters of the three probes as a function of the mole fraction of the detergent in mixed aggregates (membranes and/or micelles), X_e.

X_e was calculated according to (see (5))

$$X_e = \frac{c_{D,e}}{c_L + c_{D,e}} = \frac{Kc_D}{1 + K(c_L + c_D)}, \qquad (2)$$

with c_D denoting the total detergent concentration, $c_{D,e}$ the concentration of aggregate-bound detergent, c_L the lipid concentration (assumed to be completely aggregate-bound), and the mole-ratio partition coefficient K. For $C_{12}EO_8$, we used K = 6/mM (5); variations of $K(X_e)$, particularly between bilayers and micelles, have no significant effect on the plot. This system forms mixed membranes at X_e up to X_e^{sat} = 0.31, a coexistence of mixed membranes with wormlike micelles in the range between X_e^{sat} and X_e^{sol} = 0.62, only wormlike micelles at X_e^{sol}, and a gradual transition between wormlike and small quasispherical micelles centered at $X_e \approx 0.85$ ((35), see *vertical grid lines* in Fig. 2).

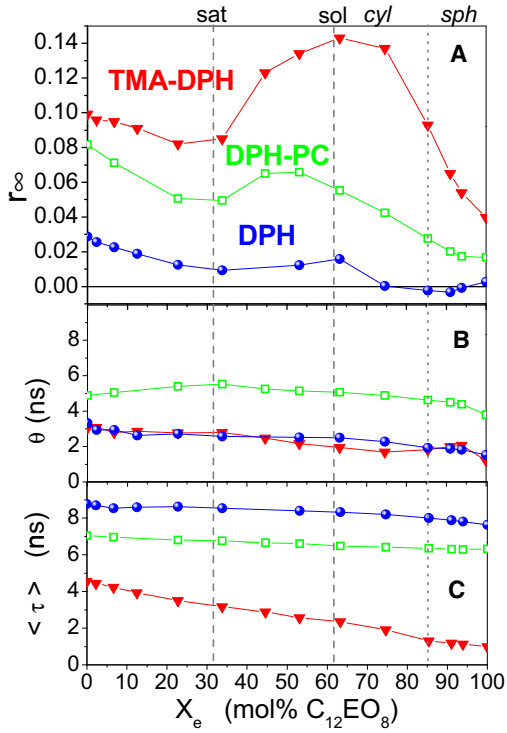

FIGURE 2 Fluorescence properties of DPH derivatives in mixtures of POPC and $C_{12}EO_8$ at 20°C as a function of the mole fraction of detergent in mixed aggregates, X_e (see text). Measurements of limiting anisotropy (*A*, r_∞), effective rotational correlation time (*B*, θ), and average lifetime (*C*, $\langle\tau\rangle$) of DPH (*spheres*), TMA-DPH (*down-triangles*), and DPH-PC (*squares*). (*Vertical grid lines*) Pseudophase boundaries of solubilization (*dashed*) and the midpoint of a broad transition from cylindrical (*cyl*) to spherical (*sph*) micelles (*dotted*) (35).

Inspection of Fig. 2 *A* reveals immediately that the phase boundaries correlate with break points in the $r_\infty(X_e)$ curves of all three probes. Addition of $C_{12}EO_8$ into membranes causes a disordering represented by decreasing r_∞. A local minimum of r_∞ is obtained at the maximal detergent content in membranes, at X_e^{sat}. The progressive formation of wormlike micelles between X_e^{sat} and X_e^{sol} increases r_∞ of all DPH probes. After a local maximum at X_e^{sol}, the micelles are gradually converted into small, quasispherical micelles and r_∞ decreases concomitantly.

The rotational correlation times of the three probes show no break points and only minor trends. The average fluorescence lifetimes (Fig. 2 *C*) decrease weakly (DPH, DPH-PC) or significantly (TMA-DPH) with increasing detergent content. Resulting from biexponential fits of the sum of decays, these trends mainly reflect a decrease in the prefactor of the longer lifetime, $\tau_2 \approx 9$ ns. We hypothesize that absolutely lower and more strongly decreasing $\langle\tau\rangle$ of TMA-DPH reflects its higher water exposure due to a more interfacial average location and a rougher and more dynamic interface of micelles compared to membranes.

Fig. 3 shows the analogous data for mixtures of POPC with OG. An ITC solubilization experiment (Fig. 3 *A*)

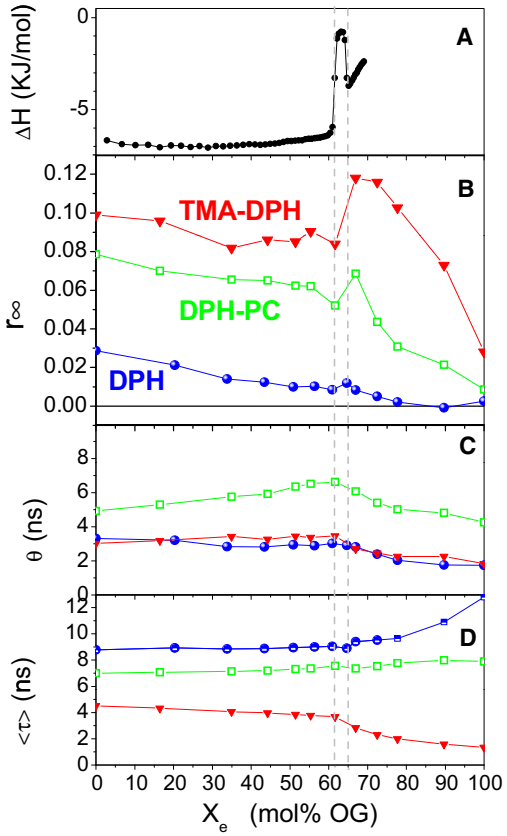

FIGURE 3 ITC solubilization experiment (*A*) and fluorescence properties of DPH derivatives (*B–D*) in mixtures of POPC with OG at 20°C as a function of the mole fraction of detergent in mixed aggregates, X_e, as calculated by Eq. 2 using $K \approx 0.1$ mM^{-1} (5). (*A*) 150 mM micellar OG was titrated into 2 mM to establish X_e^{sat} and X_e^{sol} (see *vertical grid lines*). (*B–D*) Measurements of limiting anisotropy (r_∞), effective rotational correlation time (θ), and average lifetime ($\langle\tau\rangle$) of DPH (*spheres*), TMA-DPH (*down-triangles*), and DPH-PC (*squares*).

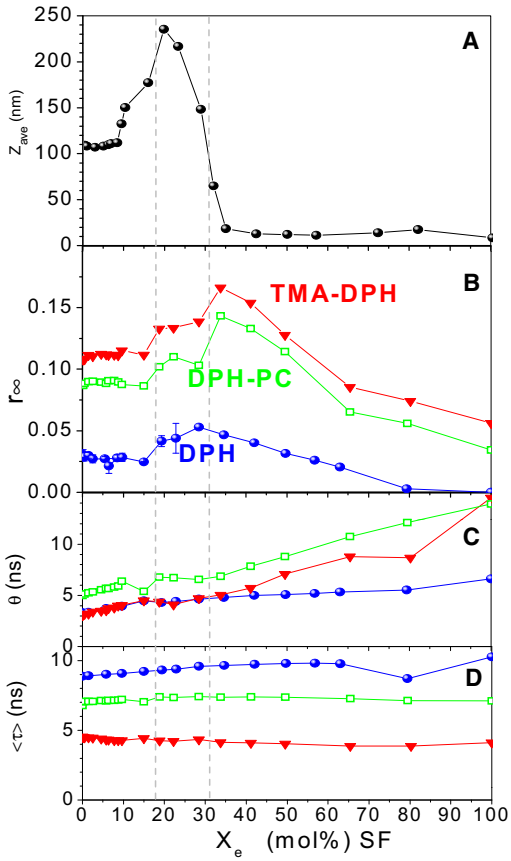

FIGURE 4 Dynamic light scattering (*A*) and DPH-fluorescence (*B–D*) data of mixtures of POPC and surfactins from *Bacillus subtilis* QST713 as a function of the effective mole fraction of the surfactin. The *z* average hydrodynamic size (*A*) confirms the onset and completion of solubilization published for a closely related system (illustrated by *gray*, *dashed*, and *vertical grid lines*). Panels *B–D* show fluorescence parameters of DPH derivatives (conditions and *symbols* are analogous to those in Figs. 2 and 3).

injecting 150 mM OG into 2 mM POPC was performed to establish the phase boundaries at 20°C, $X_e^{sat} \approx 0.61$ and $X_e^{sol} \approx 0.65$ in line with comparable references. Fig. 3, *B–D*, shows the analogous pattern as seen in Fig. 3 for $C_{12}EO_8$: $r_\infty(X_e)$ shows a minimum at the onset and maximum at the completion of solubilization. The average lifetime, $\langle\tau\rangle$, of TMA-DPH is shorter and drops upon solubilization. As for $C_{12}EO_8$, DPH-PC shows a moderate increase of θ with increasing detergent content in the membrane.

The results for surfactin lipopeptides differ qualitatively from those for typical detergents described above, particularly in the mixed membrane range at $X_e < X_e^{sat}$ (Fig. 4). The grid lines indicating X_e^{sat} and X_e^{sol} are derived from comparable literature data (5,36) and supported by the steep decrease of the average particle size (Fig. 4 *A*). SF induces only very little disordering as revealed by r_∞ of all three probes. In contrast to the detergents in Figs. 2 and 3, it causes a slight increase in θ (slower reorientation) and a slight increase of $\langle\tau\rangle$ of DPH, suggesting a slower dynamics and better screening from water in SF-containing membranes and micelles. As seen for detergents, r_∞ increases upon membrane-micelle conversion and decreases again with decreasing lipid content of the micelles.

Fig. 5 *A* compares the effects of $C_{12}EO_8$ (from Fig. 2 *A*), OG (from Fig. 3 *B*), and Triton TX-100, respectively, on r_∞ of DPH as a function of detergent concentration (log scale). The stars mark the values of r_∞ at the onset of solubilization as estimated from literature data (5) and ITC measurements (not shown) for OG/POPC, OG/POPC + Chol, and TX/POPC + Chol. For $C_{12}EO_8$ at 20°C and 10°C and TX at 20°C, r_∞ shows a local minimum at X_e^{sat} (at the *star*); the minimum is much less pronounced for OG, which has an extremely narrow coexistence range.

The curves for $C_{12}EO_8$ and OG in Fig. 5 show the following general features:

1. Membranes with higher original order may also break (start becoming solubilized) at higher order.
2. More ordered membranes are more susceptible to the disordering effect of these detergents as indicated by a steeper decrease of r_∞ (c_D).

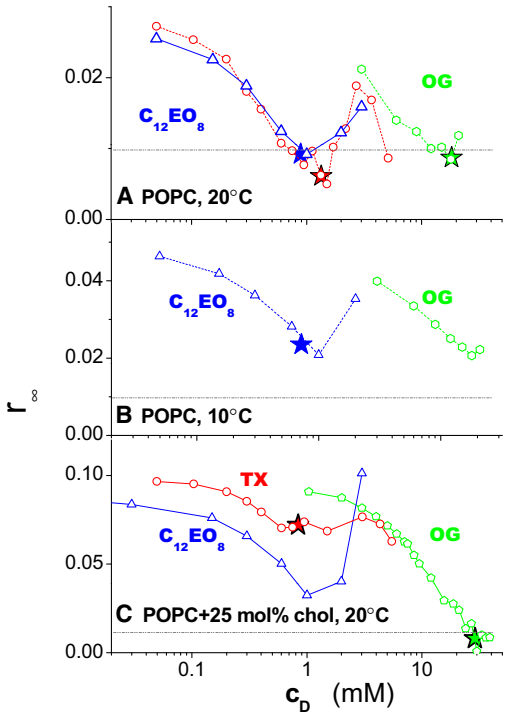

FIGURE 5 Effects of $C_{12}EO_8$ (*up-triangles*), OG (*hexa- or pentagons*), and in two cases TX (*circles*) on the limiting anisotropy, r_∞, as a function of the total surfactant concentration, c_D (the lipid concentration is ≈2 mM). The panels represent different membrane conditions, such as POPC at 20°C (*A*), POPC at 10°C (*B*), and POPC plus 25 mol % of cholesterol at 20°C (*C*). (*Dotted grid lines*) $r_\infty = 0.01$, considered critical disordering for POPC at 20°C (see Figs. 2 and 3); (*stars*) position of a curve that corresponds to the onset of solubilization for systems where this is known (see text).

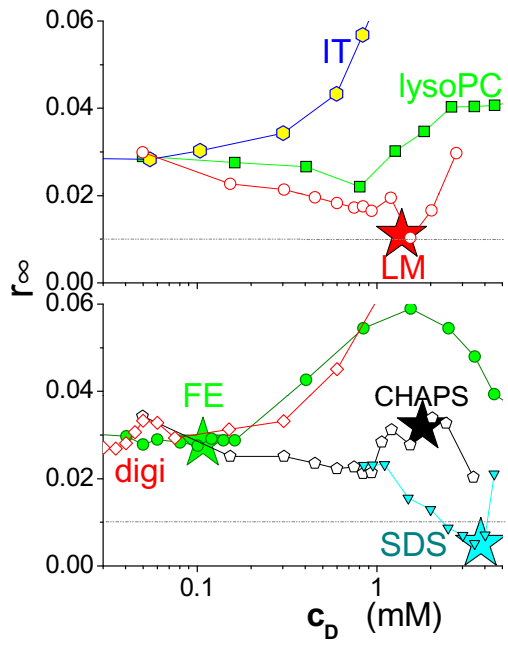

FIGURE 6 Concentration-dependent effect of surfactants on membrane order as represented by the limiting anisotropy of DPH, r_∞, as a function of the total concentration of surfactants, c_D, including dodecyl maltoside (LM, *open circles*), iturin (IT, *hexagons*), and lauroyl lysophosphatidylcholine (lysoPC, *squares*) in the top panel and sodium dodecyl sulfate (SDS, *down-triangles*), CHAPS (*pentagons*), fengycin (FE, *circles*), and digitonin (digi, *diamonds*) in the bottom panel. For LM, CHAPS, and FE, the point on the curve that corresponds to the onset of solubilization is marked by a *star*, respectively. (*Dotted grid line*) Value of $r_\infty = 0.01$ representing critical disorder in Figs. 2 and 3: it is reached by LM and SDS but not by CHAPS, FE, IT, lysoPC, and digi. All curves were recorded at ≈2 mM POPC, DPH/POPC = 1:600 mol/mol, 20°C. Note that the threshold concentrations observed here apply to ≈2 mM lipid only and are not directly comparable to the minimum inhibitory concentrations, for example.

3. The lytic concentration, X_e^{sat}, is hardly affected: higher initial order of a membrane does not protect a membrane against solubilization by a disordering detergent.
4. For each individual membrane condition, the critical order (r_∞ at the minimum) is essentially the same for $C_{12}EO_8$ and OG, respectively. It seems to be a property of the membrane primarily, not of the detergent.

For Triton, these apparent rules (which will be discussed below to apply to homogeneously disordering surfactants) do not apply, particularly in the presence of cholesterol. Then, X_e^{sat} is significantly reduced and the minimum r_∞ is substantially higher than those caused by OG or $C_{12}EO_8$.

Fig. 6 compiles the curves of r_∞ of DPH versus c_D for a number of additional surfactants. SDS and LM share the principal behavior of the detergents $C_{12}EO_8$, OG, and TX (in the absence of Chol), as illustrated in Fig. 5. They disorder the membrane to a minimum value of $r_\infty \approx$ 0.005–0.01. In contrast, CHAPS and the biosurfactants iturin (IT), fengycin (FE), digitonin (digi), and, lysoPC agree with SF in causing no or little membrane disordering so that r_∞ of DPH in POPC at 20°C remains above 0.02. Reference data about the onset of solubilization (see *stars* in Fig. 6) are available only for FE, CHAPS (37,38), and SDS (from dynamic light scattering of 65°C-equilibrated samples, not shown). Membrane solubilization by FE causes a modest increase in order. CHAPS seems to cause a slight membrane disordering that is relaxed before the onset of solubilization, which does not cause any significant further increase in r_∞.

DISCUSSION

Homogeneous membrane disordering by typical detergents

Let us first consider the detergents ($C_{12}EO_8$, OG, LM, SDS, and TX-100 in POPC) that initiate solubilization after disordering the membrane to a substantial, common degree (reflected by $r_\infty < 0.01$ in POPC at 20°C). This is, in fact, what one should expect for detergents disrupting the membrane by curvature stress. A straightforward, quantitative criterion for curvature strain (39) has been derived from Israelachvili's packing parameter concept (40), expressing the half-thickness of the hydrophobic core of the membrane, ℓ, as

$$\ell = \frac{X_S^b v_S + \left(1 - X_S^b\right) v_L}{X_S^b A_S + \left(1 - X_S^b\right) A_L}. \quad (3)$$

X_S^b denotes the mole fraction of surfactant in the membrane ($= X_e$ in the absence of micelles), v_S and v_L represent the partial volumes of the hydrophobic parts of surfactant and lipid, respectively, and A_S and A_L their partial areas at the interface. This equation assumes a planar bilayer and a smooth interface and represents the trivial fact that the hydrophobic parts have to fill the volume determined by the interfacial area multiplied by ℓ. A positive curvature strain is represented by a large A_S and/or small v_S so that $\ell < v_L/A_L$.

Let us use Eq. 3 to estimate the impact of $C_{12}EO_8$ and OG on ℓ of a POPC membrane. We use $v_L = 946$ Å^3 and $A_L = 65$ Å^2 for POPC, Tanford's (41) formula $v_S = n_C \times 26.9$ Å^3 + 27.4 Å^3 yielding v_S of 296 Å^3 and 243 Å^3 for $C_{12}EO_8$ ($n_C = 12$) and OG ($n_C = 8$), respectively. For interfacial areas we use the published values of 116 Å^2 for $C_{12}EO_8$ (42) and 51 Å^2 for OG (43). The predicted hydrophobic monolayer thickness, $\ell(X_S^b)$, is plotted in Fig. 7. It is intriguing that both curves reach the same value of $\ell^{sat} \approx 9$ Å at their respective $X_S^b = X_e^{sat}$ of 0.31 ($C_{12}EO_8$ (35)) and 0.61 (OG, Fig. 2 and (44,45)), when the membranes become disintegrated. It appears that at this point, the free energy of the curvature stress suffices to initiate micelle formation. Kinetically, this may proceed via transmembrane or micellar mechanisms (12), illustrating that the latter classification is independent of the one proposed here.

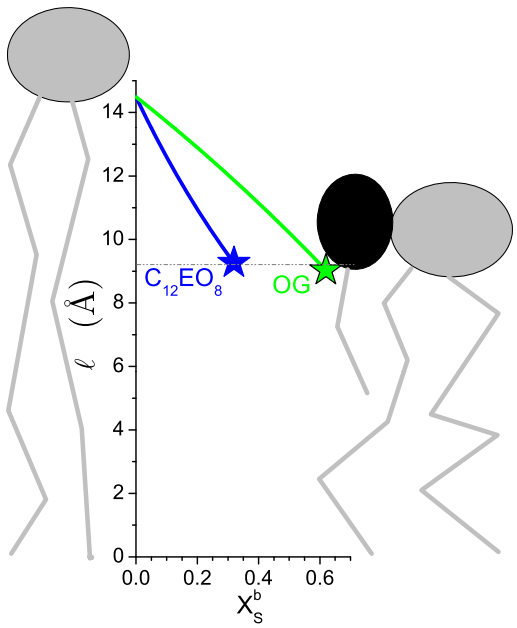

FIGURE 7 Schematic representation of the effect of detergents, $C_{12}EO_8$ and OG, on the half-thickness of the hydrophobic core of the membrane, ℓ, as predicted by Eq. 3 using parameters mentioned in the text. X_S^b denotes the mole fraction of detergent in the bilayer ($= X_e$ in the absence of micelles); the curves end at the onset of solubilization (*stars*). The agreement of ℓ at the onset of solubilization by the two detergents implies a common, critical degree of membrane disordering.

Mixtures of two or more homogeneously disordering detergents should have additive effects on membrane order as modeled elsewhere (37), whenever all interfacial areas (and hydrophobic volumes) are additive.

Summarizing, the critical disordering found here (Figs. 2 and 3, LM in Fig. 6) agrees with the theoretical prediction for a homogeneous membrane (Fig. 7) and with results of probe-free NMR and calorimetric experiments. An inhomogeneous distribution of the probes is very unlikely to substantially perturb the results given that all three probes, which should have different domain preferences (31), report the same behavior. This provides strong support for the hypothesis that these detergents initiate solubilization of a homogeneously mixed membrane at a critical curvature stress and that the latter is properly reported by r_∞ of DPH analogs. DPH anisotropy studies seem to be a new, valuable tool to detect the onset and completion of membrane solubilization by these detergents (as local minima and maxima of r_∞).

Heterogeneous perturbation and solubilization

The *Bacillus subtilis* QST713 lipopeptides surfactin, fengycin, and iturin as well as digitonin, lysolecithin, and CHAPS are all known to form micelles (i.e., to prefer aggregates with positively curved interface) and, thus, solubilize lipid membranes. In fact, where the lytic concentration, X_e^{sat}, is known, it is unusually low (0.05 for FE (38), 0.1 for CHAPS (37), 0.18 for SF (36)). This requires a particularly strong perturbation of the membrane, but this is not detected in terms of a substantially decreasing DPH order.

We propose that this lack of a substantial change in DPH order provides evidence for the system showing what we refer to as "heterogeneous perturbation": the disruption of the membrane is localized to specific membrane defects whereas the order in the bulk of the membrane is little affected.

A straightforward, possible explanation is that the detergent mixes poorly with the lipid and segregates within the membrane into detergent-rich clusters that disrupt the membrane locally whereas most of the membrane area (where also most of the DPH is located) is little affected. Failure of the detergent to mix with the lipid can also drive a segregation of the detergent from the membrane so that micelles form spontaneously in the aqueous phase (12).

Finally, one should be aware of the fact that membrane thinning by chain disordering is not the only possible way to accommodate curvature stress. A gel phase with its perfectly ordered chains cannot be disordered but matches the lateral areas of chains and headgroups by a collective tilt ($L_{\beta'}$ phase) or interdigitation of the chains. This seems uncommon for fluid membranes but NMR measurements

have provided evidence for some collective chain tilt of lipid chains caused by surfactin (9). Thinner membranes with tilted chains are likely to break at packing defects between more ordered clusters, which may also accumulate surfactant. To which extent each of these effects contributes to the phenomenon of solubilization without prior, substantial reduction of r_∞ remains to be elucidated. However, it is noteworthy that all these effects assume solubilization to be initiated in local membrane defects and we, therefore, refer to them as "solubilization by heterogeneous perturbation".

Triton mixes with POPC but gets segregated in the presence of cholesterol

The behavior of Triton illustrates that the homogeneous versus heterogeneous mode of solubilization depends on both surfactant and lipid(s). Fig. 4 shows that TX acts on POPC as expected for a homogeneously disordering detergent. However, in a membrane of POPC with 25 mol % of Chol, it behaves as a heterogeneously perturbing, segregating surfactant instead. It induces solubilization at an average r_∞ of DPH that is well above that for OG and $C_{12}EO_8$ in the same membrane and it initiates solubilization at lower c_D^{sat} than in the absence of cholesterol. The downshift in X_e^{sat} is probably even more pronounced than the one in c_D^{sat} given that cholesterol also typically decreases K (5).

This finding is in line with the fact that Triton shows unfavorable mixed pair interactions with cholesterol (46) and can, typically in contrast to OG, produce detergent-resistant membrane fragments from cholesterol-containing membranes by inducing, stabilizing, and/or coalescing ordered domains (5,47).

Functional consequences of heterogeneous perturbation

Heterogeneous perturbation as described here may account for a number of peculiar properties, such as: 1), Very low active concentration for the onset of membrane lysis (low X_e^{sat}), because the local concentration in a defect may be much higher than the average X_e. 2), Enhanced membrane selectivity (see, e.g., shift in c_D^{sat} of TX, Fig. 4), because miscibility depends on specific molecular properties whereas curvature stress is less specific. 3), Synergistic action in mixtures, if one component induces cosegregation of another. 4), Relatively high order in mixed micelles. This can be expected if the surfactant fails to disorder neighboring lipids (so that membrane curvature strain requires a tilt instead). Poor miscibility in a micelle may give rise to a bicelle or small, ellipsoidal micelle with a lipid-rich core and surfactant-rich perimeter. This may explain why antibiotic biosurfactants with a major function to kill other cells (without a need to completely dissolve them) are found to be heterogeneously perturbing, whereas classic detergents used for solubilizing other molecules in their micelles (governed by X_e^{sol}, not X_e^{sat}) are well miscible with lipids and cause homogeneous disordering.

The concept of heterogeneous perturbation supports the hypothesis of Sýkora et al. (24) that the good tolerance of digitonin by membrane proteins is related to high order (quantified by r_∞ of DPH) in the aggregates. It is also likely to apply to the triple-detergent mixture comprising dodecyl maltoside, CHAPS, and cholesteryl hemisuccinate (48). The high order retained in the membrane upon solubilization and even in the micelles may avoid a destabilization and conformational change of the protein. Enhanced contact with lipids in the core of a micelle may stabilize a protein as well (49). The two solubilization scenarios may also explain the variety of structural pathways of solubilization. Homogeneous disordering as described here is quantified in terms of a single parameter and systems sharing the same average spontaneous curvature (or ℓ) should therefore also share the same structure. It typically leads to cylindrical micelles, an aggregate of largely homogeneous, one-dimensional curvature that is intermediate between those of bilayers and spherical micelles. Heterogeneous perturbation may favor structures with different local curvatures such as perforated vesicles (10). In the case of bicelles, the limited miscibility of short-chain diacyl lipids with fluid membrane lipids gives rise to a segregation into surfactant-depleted bilayer and surfactant-rich, defect regions with pseudomicellar topologies that constitute rims of pores, bilayer fragments, or disk micelles (50).

CONCLUSIONS

Describing the activity of surfactants to permeabilize and solubilize lipid membranes, it is very useful to distinguish between homogeneously and heterogeneously membrane-perturbing surfactants.

Homogeneously disordering surfactants destroy the membrane when a critical curvature stress is reached. Their threshold concentration to lyse membranes can be estimated simply on the basis of their partition coefficient, headgroup size, and hydrophobic group volume. Our data suggest that typical synthetic detergents act by homogeneous disordering. This appears to be in line with their function to solubilize a maximum of cargo molecules in their micelles with minimum specificity.

We propose that surfactants initiating membrane lysis without a prior, substantial decrease in the limiting anisotropy, r_∞, of DPH and its analogs can be classified as heterogeneously membrane-perturbing surfactants. They disrupt membranes locally in surfactant-rich defect structures. Heterogeneous perturbation may account for the superior activity, selectivity, and mutual synergism of antimicrobial biosurfactants, such as lipopeptides and saponins, to kill target cells by permeabilizing their membrane. It may also

be favorable for membrane protein isolation because it avoids strong disordering and thinning of the protein's environment and may give rise to heterogeneous micelles with a core that is relatively rich in lipid and, possibly, sterol.

Time-resolved fluorescence anisotropy of DPH and its analogs serves to distinguish between homogeneously and heterogeneously membrane-perturbing surfactants.

Furthermore, our data suggest that the onset and completion of solubilization by membrane-disordering surfactants can be identified as local minimum and maximum of the composition-dependent, limiting anisotropy.

We are indebted to Jonathan Margolis (AgraQuest) and Sandro Keller (Universität Kaiserslautern) for helpful comments on the manuscript. We thank AgraQuest for kindly providing samples of *Bacillus* lipopeptides.

This study was supported by grants from AgraQuest and the National Science and Engineering Council of Canada.

REFERENCES

1. Ongena, M., and P. Jacques. 2008. Bacillus lipopeptides: versatile weapons for plant disease biocontrol. *Trends Microbiol.* 16:115–125.
2. Troup, G. M., S. P. Wrenn, …, T. K. Vanderlick. 2006. A time-resolved fluorescence diphenylhexatriene (DPH) anisotropy characterization of a series of model lipid constructs for the sperm plasma membrane. *Ind. Eng. Chem. Res.* 45:6939–6945.
3. Privé, G. G. 2007. Detergents for the stabilization and crystallization of membrane proteins. *Methods.* 41:388–397.
4. Heerklotz, H. H., H. Binder, and H. Schmiedel. 1998. Excess enthalpies of mixing in phospholipid-additive membranes. *J. Phys. Chem. B.* 102:5363–5368.
5. Heerklotz, H. 2008. Interactions of surfactants with lipid membranes. *Q. Rev. Biophys.* 41:205–264.
6. Heerklotz, H., H. Binder, …, G. Klose. 1994. Membrane/water partition of oligo(ethylene oxide) dodecyl ethers and its relevance for solubilization. *Biochim. Biophys. Acta.* 1196:114–122.
7. Lafleur, M., M. Bloom, …, P. R. Cullis. 1996. Correlation between lipid plane curvature and lipid chain order. *Biophys. J.* 70:2747–2757.
8. Heerklotz, H., and J. Seelig. 2000. Correlation of membrane/water partition coefficients of detergents with the critical micelle concentration. *Biophys. J.* 78:2435–2440.
9. Heerklotz, H., T. Wieprecht, and J. Seelig. 2004. Membrane perturbation by the lipopeptide surfactin and detergents as studied by deuterium NMR. *J. Phys. Chem. B.* 108:4909–4915.
10. Almgren, M. 2000. Mixed micelles and other structures in the solubilization of bilayer lipid membranes by surfactants. *Biochim. Biophys. Acta.* 1508:146–163.
11. Walter, A., P. K. Vinson, …, Y. Talmon. 1991. Intermediate structures in the cholate-phosphatidylcholine vesicle-micelle transition. *Biophys. J.* 60:1315–1325.
12. Kragh-Hansen, U., M. le Maire, and J. V. Møller. 1998. The mechanism of detergent solubilization of liposomes and protein-containing membranes. *Biophys. J.* 75:2932–2946.
13. Heerklotz, H. 2001. Membrane stress and permeabilization induced by asymmetric incorporation of compounds. *Biophys. J.* 81:184–195.
14. Bechinger, B., and K. Lohner. 2006. Detergent-like actions of linear amphipathic cationic antimicrobial peptides. *Biochim. Biophys. Acta.* 1758:1529–1539.
15. Heerklotz, H., and J. Seelig. 2001. Detergent-like action of the antibiotic peptide surfactin on lipid membranes. *Biophys. J.* 81:1547–1554.
16. Ladokhin, A. S., and S. H. White. 2001. 'Detergent-like' permeabilization of anionic lipid vesicles by melittin. *Biochim. Biophys. Acta.* 1514:253–260.
17. Shai, Y. 2002. Mode of action of membrane active antimicrobial peptides. *Biopolymers.* 66:236–248.
18. Epand, R. M., and M. Bryszewska. 1988. Modulation of the bilayer to hexagonal phase transition and solvation of phosphatidylethanolamines in aqueous salt solutions. *Biochemistry.* 27:8776–8779.
19. Hallock, K. J., D. K. Lee, and A. Ramamoorthy. 2003. MSI-78, an analogue of the magainin antimicrobial peptides, disrupts lipid bilayer structure via positive curvature strain. *Biophys. J.* 84:3052–3060.
20. Bastos, M., T. Silva, …, D. Uhríková. 2011. Lactoferrin-derived antimicrobial peptide induces a micellar cubic phase in a model membrane system. *Biophys. J.* 101:L20–L22.
21. Ludtke, S. J., K. He, …, H. W. Huang. 1996. Membrane pores induced by magainin. *Biochemistry.* 35:13723–13728.
22. Sengupta, D., H. Leontiadou, …, S. J. Marrink. 2008. Toroidal pores formed by antimicrobial peptides show significant disorder. *Biochim. Biophys. Acta.* 1778:2308–2317.
23. Lasch, J., J. Hoffmann, …, K. Gawrisch. 1990. Interaction of Triton X-100 and octyl glucoside with liposomal membranes at sublytic and lytic concentrations. Spectroscopic studies. *Biochim. Biophys. Acta.* 1022:171–180.
24. Sýkora, J., L. Bourová, …, P. Svoboda. 2009. The effect of detergents on trimeric G-protein activity in isolated plasma membranes from rat brain cortex: correlation with studies of DPH and Laurdan fluorescence. *Biochim. Biophys. Acta.* 1788:324–332.
25. Kinosita, Jr., K., and A. Ikegami. 1984. Reevaluation of the wobbling dynamics of diphenylhexatriene in phosphatidylcholine and cholesterol/phosphatidylcholine membranes. *Biochim. Biophys. Acta. Biomembr.* 769:523–527.
26. Mitchell, D. C., and B. J. Litman. 1998. Molecular order and dynamics in bilayers consisting of highly polyunsaturated phospholipids. *Biophys. J.* 74:879–891.
27. Van Der Heide, U. A., G. Van Ginkel, and Y. K. Levine. 1996. DPH is localized in two distinct populations in lipid vesicles. *Chem. Phys. Lett.* 253:118–122.
28. Lentz, B. R. 1989. Membrane 'fluidity' as detected by diphenylhexatriene probes. *Chem. Phys. Lipids.* 50:171–190.
29. Konopásek, I., J. Vecer, …, E. Amler. 2004. Short-lived fluorescence component of DPH reports on lipid-water interface of biological membranes. *Chem. Phys. Lipids.* 130:135–144.
30. Lentz, B. R. 1995. Fluorescence lifetimes of diphenylhexatriene-containing probes reflect local probe concentrations: application to the measurement of membrane fusion. *J. Fluoresc.* 5:29–38.
31. Lentz, B. R. 1993. Use of fluorescent probes to monitor molecular order and motions within liposome bilayers. *Chem. Phys. Lipids.* 64:99–116.
32. Heerklotz, H., A. D. Tsamaloukas, and S. Keller. 2009. Monitoring detergent-mediated solubilization and reconstitution of lipid membranes by isothermal titration calorimetry. *Nat. Protoc.* 4:686–697.
33. Keller, S., H. Heerklotz, and A. Blume. 2006. Monitoring lipid membrane translocation of sodium dodecyl sulfate by isothermal titration calorimetry. *J. Am. Chem. Soc.* 128:1279–1286.
34. Lakowicz, J. R. 2006. Principles of Fluorescence Spectroscopy. Springer, Boston, MA.
35. Heerklotz, H., H. Binder, …, A. Blume. 1997. Lipid/detergent interaction thermodynamics as a function of molecular shape. *J. Phys. Chem. B.* 101:639–645.
36. Heerklotz, H., and J. Seelig. 2007. Leakage and lysis of lipid membranes induced by the lipopeptide surfactin. *Eur. Biophys. J.* 36: 305–314.
37. Beck, A., A. D. Tsamaloukas, …, H. Heerklotz. 2008. Additive action of two or more solutes on lipid membranes. *Langmuir.* 24:8833–8840.

38. Patel, H., C. Tscheka, …, H. Heerklotz. 2011. All-or-none membrane permeabilization by fengycin-type lipopeptides from *Bacillus subtilis* QST713. *Biochim. Biophys. Acta.* 1808:2000–2008.

39. Heerklotz, H., and A. Blume. 2012. Detergent interactions with lipid bilayers and membrane proteins. *In* Comprehensive Biophysics, Vol. 5, Chapter 29. L. Tamm, editor.; Elsevier, Dordrecht, The Netherlands. In press.

40. Israelachvili, J. N. 1991. Intermolecular and Surface Forces. Academic Press, London, UK.

41. Tanford, C. 1980. The Hydrophobic Effect: Formation of Micelles and Biological Membranes. Wiley, New York.

42. Lantzsch, G., H. Binder, and H. Heerklotz. 1994. Surface area per molecule in lipid/C12En membranes as seen by fluorescence resonance energy transfer. *J. Fluoresc.* 4:339–343.

43. Wenk, M. R., T. Alt, …, J. Seelig. 1997. Octyl-β-D-glucopyranoside partitioning into lipid bilayers: thermodynamics of binding and structural changes of the bilayer. *Biophys. J.* 72:1719–1731.

44. Paternostre, M., M. Viard, …, R. Blumenthal. 1997. Solubilization and reconstitution of vesicular stomatitis virus envelope using octylglucoside. *Biophys. J.* 72:1683–1694.

45. Wenk, M., and J. Seelig. 1997. Vesicle-micelle transformation of phosphatidylcholine/octyl-β-D-glucopyranoside mixtures as detected with titration calorimetry. *J. Phys. Chem. B.* 101:5224–5231.

46. Tsamaloukas, A., H. Szadkowska, and H. Heerklotz. 2006. Nonideal mixing in multicomponent lipid/detergent systems. *J. Phys. Condens. Matter.* 18:S1125–S1138.

47. Heerklotz, H. 2002. Triton promotes domain formation in lipid raft mixtures. *Biophys. J.* 83:2693–2701.

48. Grisshammer, R. 2006. Understanding recombinant expression of membrane proteins. *Curr. Opin. Biotechnol.* 17:337–340.

49. Banerjee, P., J. B. Joo, …, G. Dawson. 1995. Differential solubilization of lipids along with membrane proteins by different classes of detergents. *Chem. Phys. Lipids.* 77:65–78.

50. Luchette, P. A., T. N. Vetman, …, J. Katsaras. 2001. Morphology of fast-tumbling bicelles: a small angle neutron scattering and NMR study. *Biochim. Biophys. Acta.* 1513:83–94.